

AD _____
(Leave blank)

Award Number: W81XWH-07-1-0218

TITLE: Non-Invasive Nanodiagnostics of Cancer (NINOC)

PRINCIPAL INVESTIGATOR: Alexander Kabanov, Ph.D.

CONTRACTING ORGANIZATION: University of Nebraska
Omaha, NE 68198-7835

REPORT DATE: April 2010

TYPE OF REPORT: Annual

PREPARED FOR: U.S. Army Medical Research and Materiel Command
Fort Detrick, Maryland 21702-5012

DISTRIBUTION STATEMENT: (Check one)

- ☒ Approved for public release; distribution unlimited
- ☐ Distribution limited to U.S. Government agencies only;
report contains proprietary information

The views, opinions and/or findings contained in this report are those of the author(s) and should not be construed as an official Department of the Army position, policy or decision unless so designated by other documentation.

REPORT DOCUMENTATION PAGE				Form Approved OMB No. 0704-0188	
Public reporting burden for this collection of information is estimated to average 1 hour per response, including the time for reviewing instructions, searching existing data sources, gathering and maintaining the data needed, and completing and reviewing this collection of information. Send comments regarding this burden estimate or any other aspect of this collection of information, including suggestions for reducing this burden to Department of Defense, Washington Headquarters Services, Directorate for Information Operations and Reports (0704-0188), 1215 Jefferson Davis Highway, Suite 1204, Arlington, VA 22202-4302. Respondents should be aware that notwithstanding any other provision of law, no person shall be subject to any penalty for failing to comply with a collection of information if it does not display a currently valid OMB control number. PLEASE DO NOT RETURN YOUR FORM TO THE ABOVE ADDRESS.					
1. REPORT DATE (DD-MM-YYYY) 04/30/2010		2. REPORT TYPE Annual		3. DATES COVERED (From - To) 04/01/2009 - 03/31/2010	
4. TITLE AND SUBTITLE Non-Invasive Nanodiagnostics of Cancer				5a. CONTRACT NUMBER W81XWH-07-1-0218	
				5b. GRANT NUMBER	
				5c. PROGRAM ELEMENT NUMBER	
6. AUTHOR(S) Alexander Kabanov Email: akabanov@unmc.edu				5d. PROJECT NUMBER	
				5e. TASK NUMBER	
				5f. WORK UNIT NUMBER	
7. PERFORMING ORGANIZATION NAME(S) AND ADDRESS(ES) University of Nebraska 987835 Nebraska Medical Center Medical Center, Sponsored Omaha, NE 68198-7835 Programs Administration				8. PERFORMING ORGANIZATION REPORT NUMBER	
9. SPONSORING / MONITORING AGENCY NAME(S) AND ADDRESS(ES) USA Med Research ACQ Activity 820 Chandler St. Fort Derrick, MD				10. SPONSOR/MONITOR'S ACRONYM(S) DOD	
				11. SPONSOR/MONITOR'S REPORT NUMBER(S)	
12. DISTRIBUTION / AVAILABILITY STATEMENT Approved for public release; distribution unlimited.					
13. SUPPLEMENTARY NOTES					
14. ABSTRACT This project seeks to develop noninvasive diagnostics to detect cancer in its earliest, most easily treatable, pre-symptomatic stage. Innovative imaging nanomaterials and delivery technologies are employed to target, label, and detect the cancer cells within the body at sites which are normally inaccessible to conventional diagnostic methods. The hydrophilic polymer nanogels of core-shell emission computed tomography, computer tomography, magnetic resonance, or luminescence detection. The surface of the nanogels is modified with genetically engineered antibody fragments to target the surface of cancer cells and provide site-specific delivery of the nanogels to tumors in the body.					
15. SUBJECT TERMS Noninvasive diagnostics to detect cancer					
16. SECURITY CLASSIFICATION OF:			17. LIMITATION OF ABSTRACT UU	18. NUMBER OF PAGES 21	19a. NAME OF RESPONSIBLE PERSON Keith Sutton
a. REPORT U	b. ABSTRACT U	c. THIS PAGE U			19b. TELEPHONE NUMBER (include area code) 402-559-3455

Table of Contents

	<u>Page</u>
Introduction.....	4
Body.....	5
Key Research Accomplishments.....	18
Reportable Outcomes.....	19
Conclusion.....	19
References.....	20

INTRODUCTION

To improve the detection and treatment of cancer, tumor-specific targeting has been proposed using a variety of targeting moieties such as folic acid, transferrin, RGD-peptides, antibodies or their fragments. A typical targeting method is to use antibodies to target cancer cellular markers. Maximal tumor targeting with minimal background or minimal exposure of normal organs is the goal for the clinical application of monoclonal antibodies (MAbs) for cancer diagnosis and therapy. MAbs and their fragments are of particular interest due to their high specificity for their epitopes, as well as wide variety of possible target structures. In addition, successful development of genetically engineered humanized antibody fragments reduces the problems with immune responses against mouse antibodies [1].

Tumor-associated mucines have been implicated in the pathogenesis of many cancers. Tumor-associated glycoprotein (TAG-72) is a panadeno-carcinoma antigen, which is expressed by majority of primary and metastatic human adenocarcinomas. It has been demonstrated that TAG-72 is expressed on about 85% of human adenocarcinomas such as colon, breast, pancreatic, ovarian, prostate, non-small cell lung, and gastric cancers and is not expressed in normal adult tissues except secretory endometrial tissues [2].

The murine MAb CC49 recognizes the sialyl-Tn and sialyl-T epitopes [3], which are disaccharide carbohydrate antigens present on mucin-like glycoproteins, including TAG-72. MAbs CC49 exhibit high reactivity to gastric, pancreatic and colon adenocarcinomas. Due to the high specificity and strong immunoreactivity to target antigen, CC49 antibody has entered in clinical trials for the imaging and treatment of various carcinomas [4]. These data suggest that anti-TAG72 antibodies can be exploited in rational design of the targeted nanogels to improve the selectivity of colorectal cancer imaging.

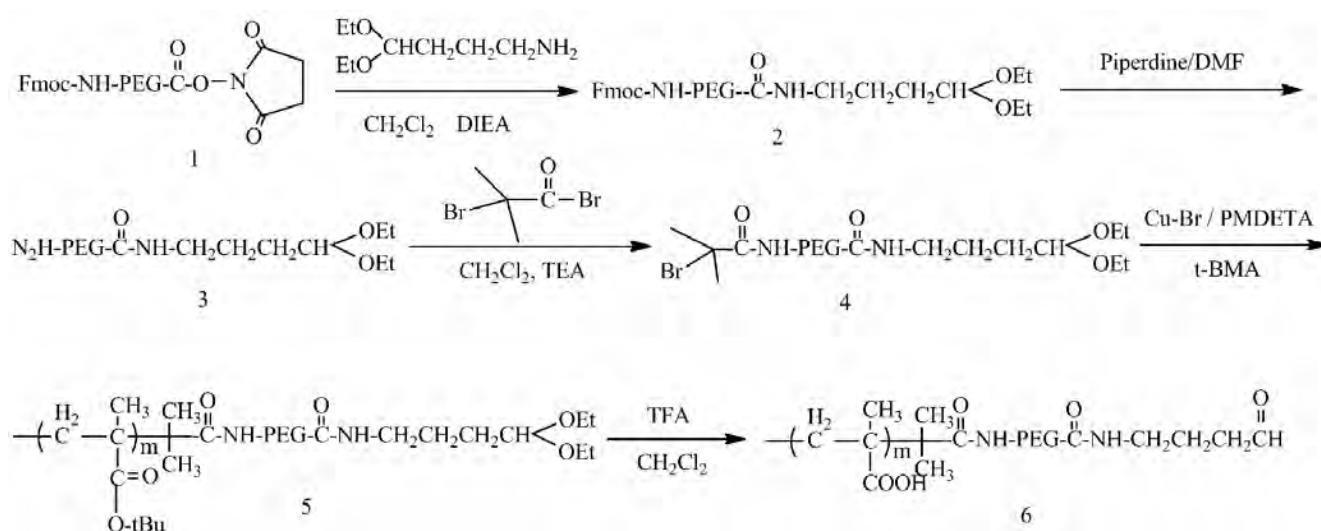
The simple and controlled method of the conjugation of various proteins to the nanoparticle surface can still pose a significant challenge. One of the attractive approach is to use the aldehyde functionalized polymer and N-terminal amino group of proteins for formation of stable secondary amino linkage via reductive amination [5]. The PEG possessing a terminal aldehyde group, also called as “second-generation” PEGylation reagent, is widely used for conjugation with proteins in biomedical field [6-8].

BODY OF REPORT

This section describes the efforts devoted by the program team to meet the major technical objectives that were: 1) develop the procedures for the synthesis of nanogels with terminal reactive groups on the surface; 2) conjugate antibodies to a nanogel surface; 3) demonstrate specificity of the antibody-nanogels conjugates to immunogen; 4) test the tumor-targeting capabilities of CC49-modified nanogels in vivo.

Synthesis of block copolymers

Well-defined block copolymers were synthesized by atom transfer radical polymerization (ATRP) [7]. The general scheme of synthesis of PEG-*b*-PMA block copolymers with terminal aldehyde group by ATRP is outlined in **Scheme 1**. The synthetic procedure included three parts: 1) the synthesis of macroinitiator **4**, 2) the synthesis of precursor block copolymer **5**, acetal-PEG-*b*-P*t*BMA, by ATRP and 3) the deprotection of precursor leading to the formation of aldehyde-PEG-*b*-PMA. Each of these steps produced stable intermediates, which were characterized by ¹H-NMR (**Figure 1**).



Scheme 1. Synthesis of aldehyde-PEG-*b*-PMA block copolymer.

First, the macroinitiator **4** was synthesized from Fmoc-PEG-NHS by introduction of acetal group and amidation of the product **3** in the presence of 2-bromoisobutyryl bromide. In order to introduce the acetal group, Fmoc-PEG-NHS **1** was reacted with the excess 4-aminobutylaldehyde diethyl acetal in dichloromethane in the presence of DIEA. The

disappearance of chemical shift of methylene group (2.8 ppm) of NHS in Fmoc-PEG-NHS as well as the presence of methylene group (3.4 ppm) and methyl group (1.2 ppm) of acetal in ^1H -NMR spectra of intermediate **2** indicated the successful introduction of acetal groups (**Figure 1.2**). The peak at 3.61 ppm corresponded to the typical protons of PEG chain. The deprotection of the Fmoc units of intermediate **2** was carried out using 20% piperidine/DMF and was proceeded completely, as confirmed by the disappearance of the specific protons of Fmoc group (7.2-7.8 ppm, 5.3 ppm) in the ^1H -NMR spectra (**Figure 1.3**). Then terminal amino group of intermediate product **3** reacted with 2-bromoisobutyryl bromide via amidation reaction. After thorough purification, the macroinitiator **4** was analyzed by ^1H -NMR (**Figure 1.4**). The singlet at 1.96 ppm, which belongs to the protons of $\text{Br-C}(\text{CH}_3)_2-$, indicated the successful synthesis the macroinitiator **4**. The second step of the synthetic procedure was the polymerization of *tert*-butyl methacrylate by ATRP, which was initiated by macroinitiator **4** [8]. The presence of backbone protons of PMA chains (1.65 and 1.00 ppm) and *tert*-butyl group (1.4 ppm) in ^1H -NMR spectrum of product **5** confirmed the successful polymerization (**Figure 1.5**). There were no unpolymerized *tert*-butyl methacrylate remained in the purified diblock copolymer **5**, as determined by GPC (data not shown). The average molar composition of diblock copolymer was quantitatively determined by comparing the integrated areas of *tert*-butyl and PEG groups (**Table 1**). In order to obtain the final block copolymer **6**, the hydrolysis of copolymer **5** was carried out in the acidic condition, which allows removing of *tert*-butyl and acetal groups simultaneously. This deprotection reaction proceeded completely, as confirmed by the disappearance of the peaks attributed to the *tert*-butyl and acetal units in the ^1H NMR spectra of aldehyde-PEG-*b*-PMA (**Figure 1.6**). It should be noted that the degree polymerization of PMA did not change upon the hydrolysis.

The chemical compositions and molecular weights of the resulting block copolymers with terminal aldehyde group are summarized in **Table 1**. The aldehyde-PEG-*b*-PMA diblock copolymers, comprising the constant PEG block (114 repeating units) and anionic segment of various length (56, 75, and 133 repeating units), were synthesized. Diblock copolymer samples are denoted as PEG(*x*)-*b*-PMA(*y*), where *x* and *y* represent the degree of polymerization of the PEG and PMA segments, respectively. The GPC profiles confirmed the synthesis of uniformed polymers with narrow molecular distribution, M_w/M_n (**Table 1**). The analysis of the samples showed very good agreement between the molecular weight determined by GPC and ^1H -NMR.

Altogether, the well-defined amphiphilic PEG-*b*-PMA diblock copolymers with terminal aldehyde group were successfully synthesized by ATRP technique.

Table 1. Physicochemical characteristics of aldehyde-PEG-*b*-PMA diblock copolymers

Composition	Mn by NMR	Mn by GPC	M_w/M_n
PEG(114)- <i>b</i> -PMA(56)	9,337	9,076	1.15
PEG(114)- <i>b</i> -PMA(75)	10,781	10,105	1.21
PEG(114)- <i>b</i> -PMA(133)	15,189	14,875	1.25

Mw: average molecular weight; Mw/Mn: polydispersity

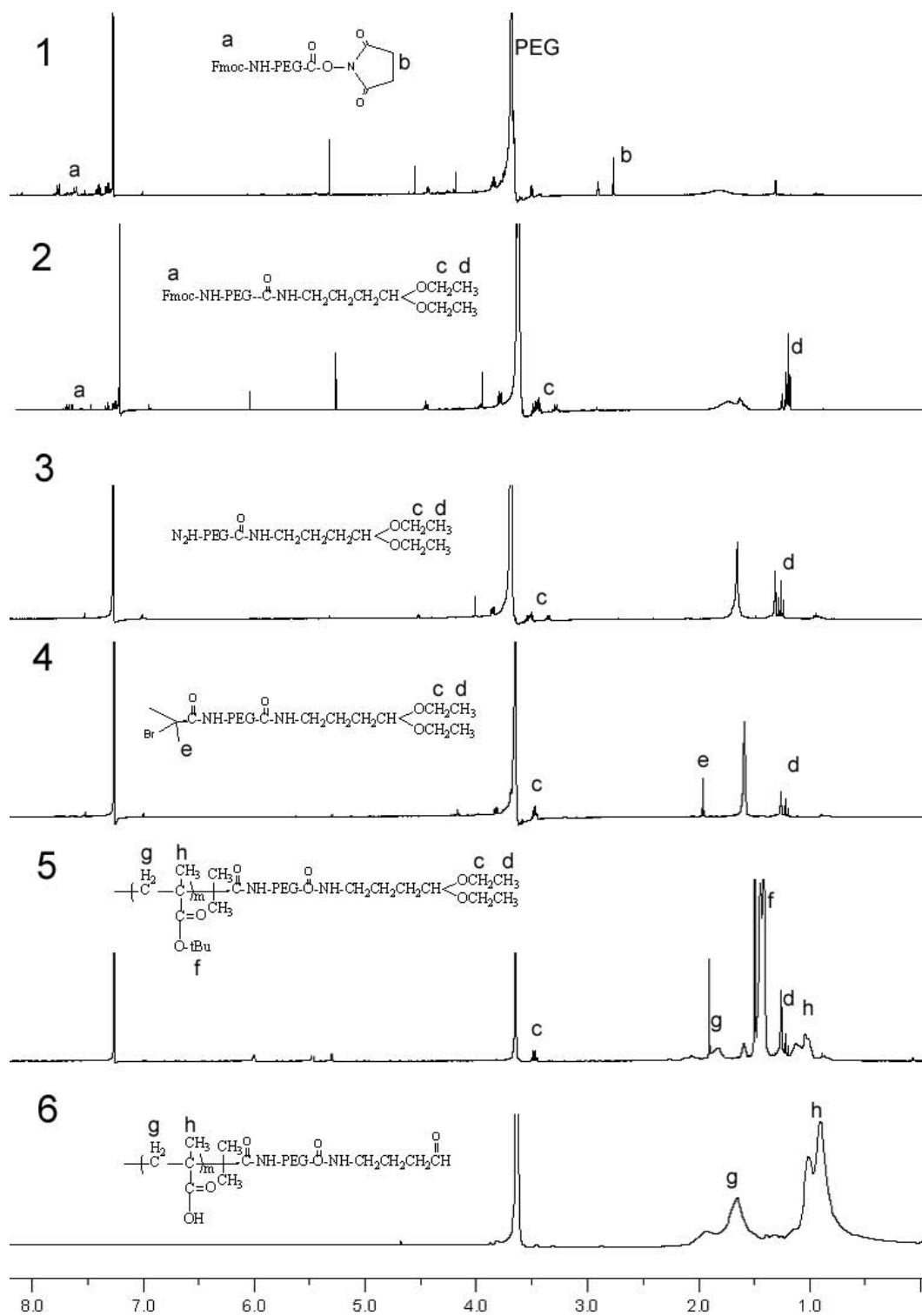


Figure 2. ^1H NMR spectra of the intermediates and final aldehyde-PEG-*b*-PMA block copolymer. The numbers are consistent with those in the **Scheme 1**. The solvents are CDCl_3 (1-5) and D_2O (6), respectively.

Synthesis of surface functionalized nanogels

Cross-linked nanogels with aldehyde functional groups, *cl*-PEG-*b*-PMA, were prepared by template-assisted method using a two-step process, which includes 1) condensation of aldehyde-PEG-*b*-PMA copolymers with Ca^{2+} ions into spherical self-assembled block ionomer complexes (BIC) and 2) cross-linking reaction of BIC templates by bifunctional agents using the procedure described in our previous reports and publications [9-11].

The BIC formation of aldehyde-PEG-*b*-PMA block copolymers with Ca^{2+} ions was determined by an increase of turbidity of the system and their particle size [10]. The **Figure 3** presents the turbidity and particle size of PEG-*b*-PMA/ Ca^{2+} complexes as a function of the charge ratio in the mixture, Z . The latter is expressed as $Z = C_m \cdot n / C_i$, where C_m is Ca^{2+} molar concentration, n is the valence of the metal ion, and C_i is the molar concentration of the carboxylate groups of PMA chains at a given pH. Notably, the complexation behavior of PEG-*b*-PMA copolymers with condensing agent was strongly dependent on the length of the ionic PMA segments of the block ionomer (**Figure 3A**). Thus, the onsets of BIC formation in PEG(114)-*b*-PMA(133)/ Ca^{2+} , PEG(114)-*b*-PMA(75)/ Ca^{2+} and PEG(114)-*b*-PMA(56)/ Ca^{2+} mixtures were observed in the vicinity of $Z = 1.0$, 1.3 and 1.5, respectively, as manifested by an increase in the turbidity of the system. The presence of higher content of hydrophilic PEG segments in the PEG-*b*-PMA copolymers affected the onset of self-assembly in the PEG-*b*-PMA/ Ca^{2+} mixtures which is shifted towards higher concentration of condensing agent (or higher charge ratio Z). The particle size of the resulting BICs was determined by dynamic light scattering (DLS) at the onset of self-assembly of PEG-*b*-PMA block copolymers with Ca^{2+} ions (**Figure 3B**). The formation of narrow distributed particles with hydrodynamic diameter less than 80 nm (PDI <0.1) was detected. As the amount of condensing agent increased, the particle sizes of PEG-*b*-PMA/ Ca^{2+} complexes were slightly increased. Notably, the BIC of all prepared copolymers were stable in the aqueous solutions over the entire range of the charge ratios studied in this work. These block ionomer-metal complexes can be considered as a special type of the copolymer with neutralized, water-insoluble segments from the polyion-metal complex and water-soluble PEG chains. Overall, these data suggest that the relative ratio of neutralized and polyether segments determined the solution properties of the complexes.

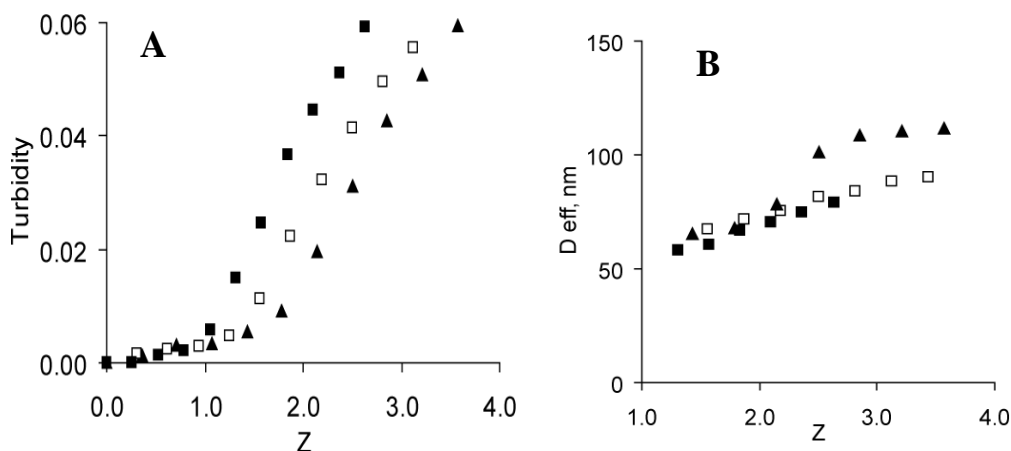


Figure 3. Turbidity of the PEG-*b*-PMA/Ca²⁺ systems as a function of the charge ratio in the mixture, Z : (■) PEG(114)-*b*-PMA(133), (□) PEG(114)-*b*-PMA(75) and (▲) PEG(114)-*b*-PMA(56).

The BIC formed between PEG-*b*-PMA polymer and Ca²⁺ ions were further utilized as “core-shell” templates for the synthesis of cross-linked nanogels with aldehyde functional groups. Cross-linking of the core of the PEG-*b*-PMA/Ca²⁺ complexes was achieved via condensation reactions between the carboxylic groups of PMA chains and the amine functional groups of ethylenediamine in the presence of a water-soluble carbodiimide, EDC. The resulting *cl*-PEG-*b*-PMA nanogels possessed the hydrogel-like behavior upon a change of pH and ionic strength of solution [9, 10]. The particle size and net negative ζ -potential of the nanogels were reversibly and considerably increased with increase of pH (**Figure 4A, 5B**). Such swelling behaviors were induced by the ionization of the carboxylic groups of the PMA chains and increasing of osmotic pressure due to the penetration of the counterions into the volume of nanogels. It should be noted that cross-links may take place in PEG shell as a side reaction between aldehyde and amino groups, forming unstable imines under experimental conditions [12,13]. Anyhow, the DNPH colorimetric assay revealed sufficient amount of free aldehyde groups in nanogels for further conjugation with mAbs.

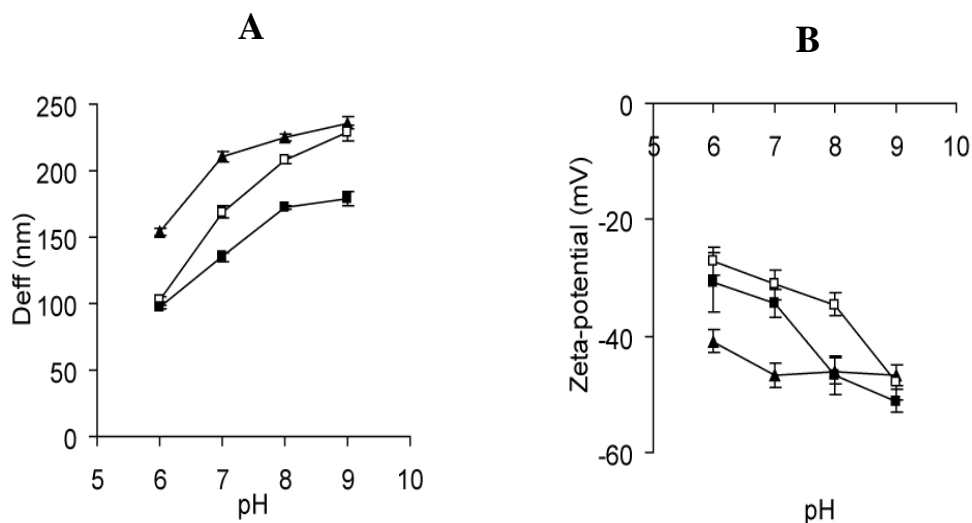


Figure 4. Physicochemical characteristics of aldehyde-functionalized *cl*-PEG-*b*-PMA nanogels. **(A)** Effective diameter (D_{eff}) and **(B)** ζ -potential of *cl*-PEG-*b*-PMA nanogels with 20% targeted degree of cross-linking as a function of pH. (■) *cl*-PEG(114)-*b*-PMA(133), (□) *cl*-PEG(114)-*b*-PMA(75) and (▲) *cl*-PEG(114)-*b*-PMA(56). Effective diameter denotes averaged value calculated from three measurements performed on each sample.

The size and morphology of cross-linked nanogels were further characterized by tapping-mode AFM. This technique allows visualization of the entire particles and yields their heights and widths. The typical AFM images of *cl*-PEG-*b*-PMA nanogels showed spherical nanoparticles with a narrow distribution in size (**Figure 5**). The aspect ratio, diameter versus height, shows the “softness” of *cl*-PEG-*b*-PMA nanogels (**Table 2**). It should be noted that usually tapping-mode AFM detects the lower values for the height of the soft material due to the elastic deformation of material and drying process (AFM in air), but higher numbers for the width as a result of tip convolution effect. Also, prepared negatively charged *cl*-PEG-*b*-PMA nanogels were deposit on positively charged APS-mica. Therefore, the electrostatic interactions between nanogels and APS-mica might give an additional flattening of the nanogel particles. Nevertheless, *cl*-PEG(114)-*b*-PMA(133) nanogels had the smallest height and diameter, which is consistent with DLS results. This nanogel had relatively less weight fraction of the hydrophilic PEG chains ($f_{EG} = 0.26$) in comparison with other prepared nanogels. The largest nanoparticles were observed in *cl*-PEG(114)-*b*-PMA(56), which had bigger a weight fraction of PEG blocks ($f_{EG} = 0.45$). These data were in agreement with the expected flexible, shape-adaptable character of these nanostructures imparted by the “softness” of material. Overall, the aldehyde-

functionalized nanogels displayed volume transitions at the nanosized scale in response to changes in pH.

Table 2. Dimensions of *cl*-PEG-*b*-PMA nanogels

Nanogels	f_{EG}^a	AFM			DLS
		H_{av}^b , nm	W_{av}^c , nm	Aspect ratio (W_{av}/H_{av})	D_{eff} (nm) ^d
<i>cl</i> -PEG(114)- <i>b</i> -PMA(56)	0.45	13.2 ± 0.2	162.7 ± 2.9	12.4	210.3
<i>cl</i> -PEG(114)- <i>b</i> -PMA(75)	0.38	7.2 ± 0.1	96.0 ± 0.9	13.3	168.6
<i>cl</i> -PEG(114)- <i>b</i> -PMA(133)	0.26	5.7 ± 0.1	85.5 ± 0.3	15.0	135.2

^a The weight fraction of PEG blocks

^b Number-averaged heights (H_{av}) of the nanogels

^c Number-averaged widths (W_{av}) of the nanogels

^d Effective diameter at pH 7.0

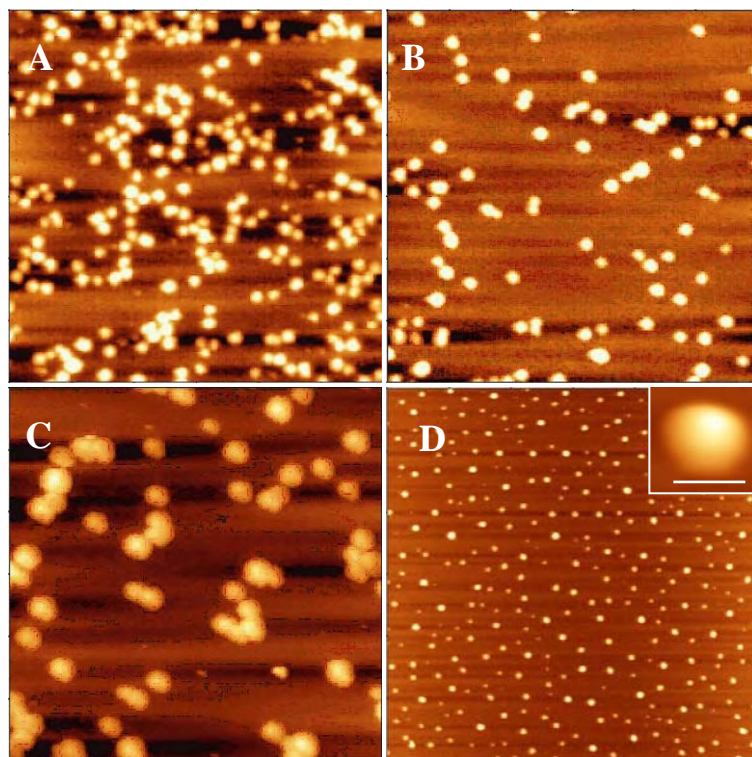


Figure 5. Tapping-mode AFM images of nanogels and mAb-nanogels deposited from aqueous solutions on the APS-mica. (A) *cl*-PEG(114)-*b*-PMA(133), (B) *cl*-PEG(114)-*b*-PMA(75), (C) *cl*-PEG(114)-*b*-PMA(56), and (D) CC49-nanogel. Scan size in 3 μ m. The inserts show 3D image of the same nanogels. Bar equals 40 nm.

Conjugation of monoclonal antibody to a nanogel surface

c-PEG(114)-*b*-PMA(133) nanogel was chosen as a platform for further conjugation of antibody to a nanogel surface using reductive amination reaction. The specific targeting ligand to TAG-72, monoclonal antibody CC49, was successfully conjugated to nanogels via aldehyde functional groups in the presence of sodium cyanoborohydride. The reaction proceeded via an intermediate imine (Schiff base) which was in equilibrium with their free forms and highly pH dependent [5, 13]. The reduction of Schiff base was irreversible and led to formation of chemically stable bond. The purified mAb-nanogels were obtained after the size exclusion chromatography on Sepharose CL-6B. It should be noted that the purification of reaction mixture allowed removing all unbound mAb, while unmodified and mAb-conjugated nanogels are not separated. The conjugation of CC49 to nanogels resulted in the slight decrease of particle size from 175 ± 5 nm to 159 ± 2 nm ($PDI < 0.12$). Interestingly, the ζ -potential of the CC49-nanogels was significantly decreased from -32.1 ± 3.2 mV to -17.0 ± 2.7 mV. Practically the same results were obtained for control non-specific IgG-nanogels. It is likely that the net negative charge of the mAb-nanogels was partially shielded by conjugated mAbs. The swelling behavior of mAb-nanogels was practically the same as for unmodified nanogels. The morphology of nanogels remained unchanged after their conjugation with mAb as determined by AFM in air (**Figure 5D**). The amount of conjugated mAb was evaluated by micro BCA assay and was estimated to be 100-150 μ g per mg of nanogel. The unmodified and mAb-conjugated nanogels remained stable in phosphate buffered saline (pH 7.4) in a wide range of concentrations (up to 1.5 %), exhibiting no aggregation for weeks. Interestingly, mAb-nanogels with high amount of conjugated mAb (more than 200 μ g per mg of nanogel) were aggregated over the time (days). Overall, these data demonstrated that the sufficient amount of mAb could be conjugated to the nanogels by simple method without changing morphology of the nanocarriers.

Evaluation of antigen-binding selectivity of antibody conjugated nanogels

In order to investigate the antigen-binding selectivity of mAb-nanogels, the surface plasmon resonance (SPR) measurements were performed. SPR technique has been used extensively in analyzing macromolecular interactions, including those between antibodies and their antigens. To define the specific binding of the CC49-nanogels to its targeted antigen BSM,

the BSA coated sensor chip and IgG-nanogels were used as controls [32]. SPR analysis revealed that CC49-nanogels were able to effectively recognize the immobilized BSM as seen by the strong specific binding of the targeted nanogels (**Figure 6**). However, the nanogels without targeting moiety or unspecific IgG-nanogels showed no specific binding to the BSM antigen. Also, the response of CC49-nanogles was partially attenuated by adding free CC49 either before or simultaneously with the CC49-nanogles, but the same response was not affected by adding the free IgG (not shown in figure). The association constants (K_A) as determined by real-time kinetic analysis using BIAcore for free CC49 and CC49-nanogles were 1.25×10^8 and $9.6 \times 10^7 \text{ M}^{-1}$, respectively; the dissociation constants (K_D) were 8 nM and 10.3 nM, respectively. This important result indicates that the conjugation of CC49 to the nanogels did not change its activity and kept intact binding affinity. In addition, to ensure the reproducibility of efficient conjugation, the procedure was repeated and SPR measurements provided the quite similar data. Taken together, our data suggest that as a result of decoration of the nanogels with the specific antibodies, the CC49-nanogels acquire ability for strong and specific interaction with its surface-immobilized antigen.

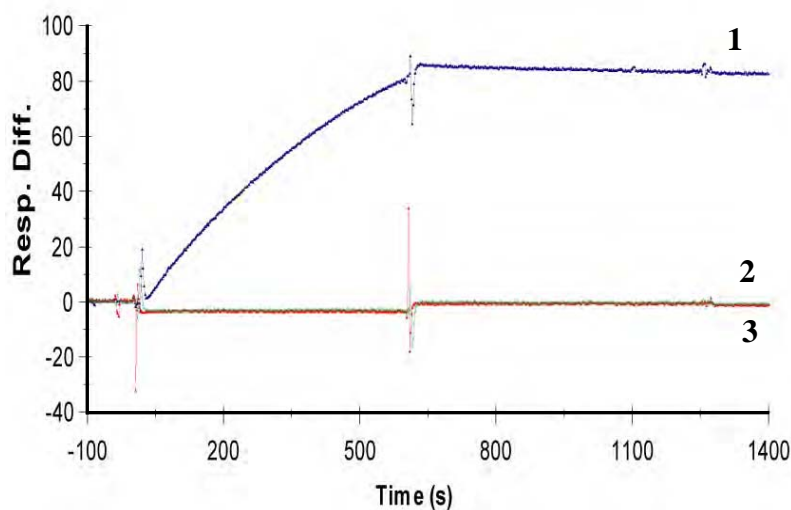


Figure 6. SPR sensorgrams of (1) CC49-nanogels, (2) IgG-nanogels, and (3) unmodified nanogels. Eluent: HBS-EP buffer, pH 7.4; flow rate: 5 $\mu\text{l/ml}$; density of BSA & BSM was approx. 0.6 ng/mm^2 per channel; sample concentration was 60 $\mu\text{g/ml}$.

Altogether, aldehyde-functional groups on the surface of the nanogels permitted the efficient conjugation with CC49 antibody for active targeting. CC49-conjugated nanogels showed high affinity to specific antigens, which could lead to recognition of TAP-72-expressing tumor cells.

Tumor detection in an animal model using CC49-labeled nanogels

The *in vivo* migration and localization of CC49-labeled nanogels were evaluated in athymic nude mice (NCr-*nu/nu*) obtained from NCI (Bethesda, MD) using optical imaging. All *in vivo* experiments were performed in accordance to animal protocol approved by UNMC IACUC and USAMRMC ACURO. Mice bearing subcutaneously implanted tumors (model **I**) were used in these experiments. A subcutaneous solid tumor was established by s.c. injection of human colon carcinoma LS-174T cells (5×10^6 in 100 μ l of culture medium) onto the back between scapulae in mice to induce tumor growth. Tumors were allowed to progress until they reach a size of about 300 mm³.

Alexa680-labeled nanogels were prepared using PEG(170)-*b*-PMA(180) block copolymer followed by conjugation with CC49 antibodies. Fluorescently labeled non-targeted nanogels and nanogels conjugated with non-specific IgG (IgG-nanogels) were used as controls. *In vivo* imaging was performed with an IVIS 200 small animal Imaging System (Xenogen, Alameda, CA) comprised of a highly sensitive, cooled CCD camera mounted in a light-tight specimen box. Images and measurements of fluorescent signals were acquired and analyzed using Living Image 2.50 software (Xenogen). An ICG filter (excitation wavelength 710-760 nm and emission wavelength 810-875 nm) was used for acquiring images *in vivo*. Background fluorescence was measured for each animal and subtracted by setting up a background measurement.

Ten minutes prior to *in vivo* imaging, three groups of LS174T tumor bearing mice (n=2-3) were given Alexa680-nanogels, nonspecific IgG-Alexa680-nanogels, and specific CC49-Alexa680-nanogels via i.v. injection, then were placed onto a warmed stage inside the camera box and were anesthetized using 1–3% isoflurane (Abbott Laboratories, North Chicago, IL). The mice were injected at a dose of 150 μ l /mouse (0.16 nmol or 0.45 nmol NIR probe/animal). Imaging time point was 1 s, and the mice were imaged at 10 min, 30 min, 1, 6, 24, 48 h after injection. Both the dorsal and ventral sides of each mouse were imaged. Animals were sacrificed at 24 and 48 h postinjection. The anatomized tissues (tumor, liver, spleen, kidney and lung) were

imaged immediately. The mean fluorescent intensity of each tissue sample was obtained by subtracting the mean fluorescent intensity of corresponding tissue from the blank mouse. The fluorescent intensities in the heart were used to reflect the fluorescent intensities in the blood. The tissue to heart ratio for fluorescence was calculated. The tissues were designated as the regions of interest (ROI).

Nanogels showed cumulative accumulation in organs and solid tumor due to its remarkably prolonged blood circulation time. The nanogels showed tumor accumulation after 1h post-injection and was maintained for an extended period. However, the biodistribution study in nude mice carrying LS174T xenografts showed the moderate uptake of targeted nanogels in the tumor site and enhanced uptake in the liver and spleen in comparison with non-targeted nanogels (**Figure 7**). Liver and spleen showed relatively high uptake of both conjugates, which is typical for entire antibodies. One of explanation of high uptake by liver could be in recognition of entire antibodies by macrophages. Based on this results we are planning to modify the surface of nanogels by fragments of CC49 (divalent and tetravalent scFv) and examine their biodistribution. Also, other reason of moderate enhance of tumor uptake is that the attachment of antibody can not be precisely controlled and as a result some portion of conjugated mAb could be inactive as well as the orientation of protein might be incompatible with receptor recognition.

In general, the accumulation of nanoparticles at tumor tissues depends on the affinity of mAb-conjugated nanogels, circulation half-life, and tumor vessel permeability. The tumor uptake could be affect by several physicochemical characteristics of nanomaterials such as particle size, net charge, coating and others. In this study, the targeted and non-targeted nanogels had different net negative charge which could also affect on tumor/liver uptake.

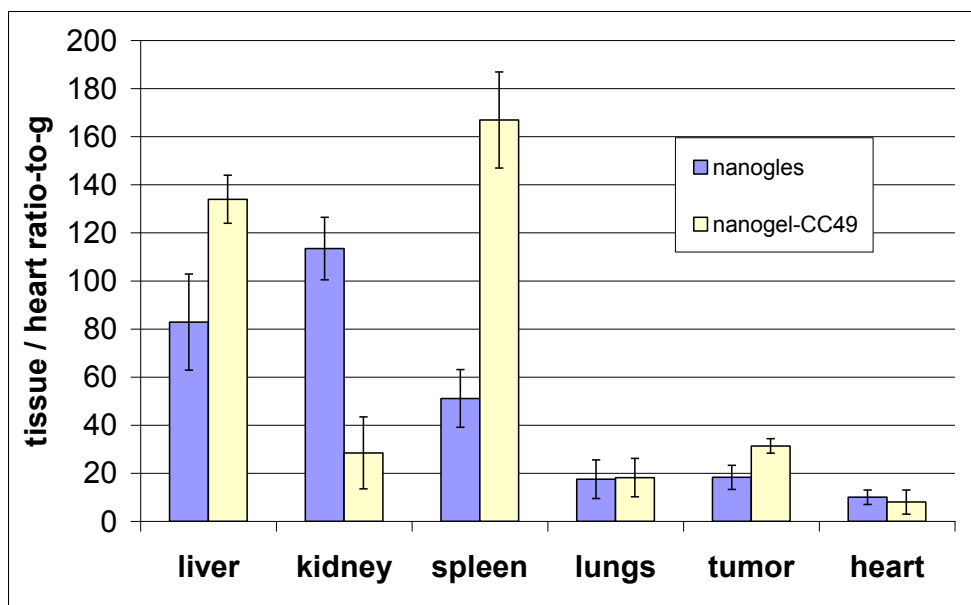


Figure 7. Tissue-to-heart ratios for the mice sacrificed 24 h after injection of Alexa-nanogels (blue bars) or CC49-Alexa680-nanogels (yellow bars). Animals were dosed with 0.45 nmol of NIR probe.

In addition, in research collaboration with group lead by Professor Yukio Nagasaki at Tsukuba Research Center for AInterdisciplinary Material Science, Graduate School of Pure and Applied Sciences, The University of Tsukuba, Japan, a novel type of PEGylated nanogels composed of the cross-linked poly[2-(N,N-diethylamino)ethyl methacrylate]-co-poly(2,2,2-trifluoroethyl methacrylate) gel core was developed and their utility as nanoprobe for ^{19}F magnetic resonance spectroscopic imaging (MRS/I) was studied. Two types of ^{19}F -MRS/I nanoprobe based on PEGylated ^{19}F -labeled pH-responsive 1) cross-linked nanogels or 2) non cross-linked, self-assembled polymeric micelles were synthesized by emulsion copolymerization, and characterized using dynamic light scattering and ^{19}F -MRS/I. Both nanogels and micelles showed remarkable on-off regulation of ^{19}F -MR signal intensity in response to a pH change from physiological pH=7.4 to tumor environment pH=6.5 and endosomal/lysosomal pH=5.5. The decrease of pH in this range resulted in the increase in the molecular motion (T_2 values) of the ^{19}F -compounds through the swelling of the nanogel cross-linked core or decomposition of the micelles non-cross-linked core. The signal noise (S/N) ratios of the PEGylated nanogels at pH=7.4, 6.5, and 5.5 calculated from phantom images were found to be ~ 0 , 7.63, and 5.75, respectively. Eventually, an appreciably enhanced S/N ratio at pH=6.5 and 5.5 was achieved,

demonstrating the utility of the PEGylated nanogels as solid tumor-specific smart ^{19}F -MRI/S nanoprobe. The results of this collaborative work were published in *Chemistry Letters*, journal of The Chemical Society of Japan.

KEY RESEARCH ACCOMPLISHMENTS

- Procedures for the synthesis of PEG-*b*-PMA block copolymers with terminal aldehyde group by atom transfer radical polymerization (ATRP) were developed.
- A series of block copolymers with different length of ionic segment was synthesized and characterized.
- Representative panel of nanogels containing aldehyde groups on the surface was synthesized using diblock copolymers of different compositions.
- The physicochemical characteristics of the nanogels (dimensions, swelling behavior) were determined.
- The CC49 antibodies to TAG72 specific to colon cancer cells were successfully attached to the nanogels.
- The physicochemical characteristics of the MAb CC49-modified nanogels (dimensions, swelling behavior) were determined by combination of different physico-chemical techniques (DLS, AFM).
- Specific binding of the MAb CC49-nanogel conjugates to bovine submaxillary mucin (BSM), which contains the epitopes recognized by CC49 antibodies, as a positive control and bovine serum albumin (BSA) as a negative control, was determined by surface plasmon resonance measurements. The binding ability of the nanogels conjugated with CC49 was compared to that of unconjugated constructs.
- The dissociation constants (K_D) for free MAb CC49 and CC49-conjugated nanogels were 8 nM and 10.3 nM, respectively.
- The CC49-labeled nanogels showed tumor accumulation after 1h post-injection which was maintained for an extended period of time (up to 72 hours).
- pH-responsive PEGylated nanogels based on cross-linked poly[2-(N,N-diethylamino)ethyl methacrylate]-co-poly(2,2,2-trifluoroethyl methacrylate) were validated as ^{19}F MRS/I nanoprobe.

REPORTABLE OUTCOMES

- The procedures for the conjugation of the antibodies to the nanogels were developed.
- Anti-TAG72 antibodies (MAb CC49) were successfully conjugated to the nanogels with aldehyde functionalities without loss in binding affinity.
- Specific recognition of antigen by CC49-modified nanogels was demonstrated.
- The feasibility of using CC49-nanogels for NIR fluorescence imaging of tumors in a xenograft animal mode was tested.

CONCLUSIONS

- Well-defined diblock copolymers of poly(ethylene glycol) and polymethacrylic acid (PEG-*b*-PMA) with aldehyde functionality were prepared using ATRP technique. The solution properties of the micellar templates can be manipulated by variation of the composition of PEG and PMA segments. Novel surface-functionalized cross-linked nanogels were synthesized by template-assisted method and successfully conjugated with mAbs. Aldehyde-functionalized surface gives an opportunity for simple and efficient conjugation with diverse proteins. Important, that the specific CC49-nanogels showed high affinity to its antigens, which confirms the intact activity of mAb during conjugation. “Proof-of –principle” optical imaging studies demonstrated that NIR-emissive CC49-modified nanogels are suitable for the detecting in vivo tumors. However, an enhanced uptake of antibody-modified nanogels in the liver and spleen was observed in comparison with non-targeted nanogels. Tumor-targeting capabilities of nanogels can be altered by using fragments of CC49 (divalent and tetravalent scFv) for modification of the surface of nanogels. These studies are currently in progress.

PUBLICATIONS AND PRESENTATIONS

1. Jong Oh Kim, Nataliya V. Nukolova,, Hardeep S. Oberoi, Alexander V. Kabanov, Tatiana K. Bronich. Block ionomer complex micelles with cross-linked cores for drug delivery. *Polymer Science Series A*, 2009, 51, 708-718.
2. Motoi Oishi , Shogo Sumitani S, Tatiana K. Bronich, Alexander V. Kabanov, Michael D. Boska, Yukio Nagasaki. Novel ¹⁹F-MRS/I nanoprobe based on pH-responsive PEGylated

- nanogel: pH-dependent ^{19}F magnetic resonance studies. *Chemistry Letters*, 2009, 38 (2), 128-129.
3. Nataliya V. Nukolova, Michael D. Boska, Alexander V. Kabanov, Tatiana K. Bronich. Cross-linked Polymer Micelles for Delivery of Imaging Agents. The 2008 Gordon Research Conference on Drug Carriers in Medicine and Biology. Big Sky, Montana, USA, August 24-29, 2008
 4. Nataliya V. Nukolova, Michael D. Boska, Alexander V. Kabanov, Tatiana K. Bronich. Polymer Micelles with Cross-linked Core for Delivery of Imaging Agents. The 6th International Nanomedicine and Drug Delivery Symposium (NanoDDS'08), Toronto, Canada, October 18-19, 2008.
 5. Nataliya V. Nukolova, Alexander V. Kabanov, Tatiana K. Bronich. Polymer Micelles for Delivery of Imaging Agents. The 40th Annual Midwest Student Biomedical Research Forum, Omaha, Nebraska, USA, February 27-28, 2009
 6. Nataliya V. Nukolova, Alexander V. Kabanov, Tatiana K. Bronich. Targeted Delivery of Polymer Nanogels. The 1st International Summer School - Nano2009. Nanomaterials and Nanotechnologies in Living Systems; Moscow Region, Russia, June 29 - July 4, 2009.
 7. Jong Oh Kim, Nataliya V. Nukolova, Zigang Yang, Alexander V. Kabanov, and Tatiana K. Bronich. Surface Functionalized Nanogels with Cross-Linked Ionic Core for Specific Tumor Targeting. The 7th International Nanomedicine and Drug Delivery Symposium (NanoDDS'09), Indianapolis, USA, October 4-7, 2009.
 8. Nataliya V. Nukolova, Surinder Batra, Alexander V. Kabanov, Tatiana K. Bronich. Preparation of Antibody-Bound Cross-Linked Micelles for Targeted Drug Delivery. The 7th International Nanomedicine and Drug Delivery Symposium (NanoDDS'09), Indianapolis, USA, October 4-7, 2009.

REFERENCES

1. T.M. Allen. Ligand-targeted therapeutics in anticancer therapy. *Nat. Rev. Cancer* 2002, 2, 750-763.
2. A. Thor, M.J. Viglione, R. Muraro, N. Ohuchi, J. Schlom, F. Gorstein, Monoclonal antibody B72.3 reactivity with human endometrium: a study of normal and malignant tissues, *Int. J. Gynecol. Pathol.* 1987, 6, 235-247.

3. H.S. Silverman, M. Sutton-Smith, K. McDermott, P. Heal, S.H. Leir, H.R. Morris, M.A. Hollingsworth, A. Dell, A. Harris, The contribution of tandem repeat number to the Oglycosylation of mucins, *Glycobiology*, 2003, 13, 265–277.
4. (a) R.F. Meredith, A.J. Bueschen, M.B. Khazaeli, W.E. Plott, W.E. Grizzle, R.H. Wheeler, J. Schlom, C.D. Russell, T. Liu, A.F. LoBuglio, Treatment of metastatic prostate carcinoma with radiolabeled antibody CC49, *J. Nucl. Med.*, 1994, 35, 1017–1022; (b) R.D. Alvarez, W.K. Huh, M.B. Khazaeli, R.F. Meredith, E.E. Partridge, L.C. Kilgore, W.E. Grizzle, S. Shen, J.M. Austin, M.N. Barnes, D. Carey, J. Schlom, A.F. LoBuglio, A Phase I study of combined modality (90)Yttrium-CC49 intraperitoneal radioimmunotherapy for ovarian cancer, *Clin. Cancer Res.* 2002, 8, 2806–2811.
5. G.T. Hermanson, *Bioconjugate Techniques*, 1st edition ed., Academic Press, San Diego, CA, 1996.
6. (a) X.S. Feng, D. Taton, E.L. Chaikof, Y. Gnanou, Bouquet-type dendrimerlike poly(ethylene oxide)s with a focal aldehyde and peripheral hydroxyls, *Biomacromolecules* 8 (2007) 2374–2378. (b) R.C. Li, R.M. Broyer, H.D. Maynard, Well-defined polymers with acetal side chains as reactive scaffolds synthesized by atom transfer radical polymerization, *J. Polym. Sci. Pol. Chem.* 44 (2006) 5004–5013. (c) H. Otsuka, Y. Nagasaki, K. Kataoka, Characterization of aldehyde-PEG tethered surfaces: Influence of PEG chain length on the specific biorecognition, *Langmuir* 20 (2004) 11285–11287.
7. K. Matyjaszewski, J.H. Xia, Atom transfer radical polymerization, *Chemical Reviews* 101 (2001) 2921–2990.
8. S. Dai, P. Ravi, C.Y. Leong, K.C. Tam, L.H. Gan, Synthesis and aggregation behavior of amphiphilic block copolymers in aqueous solution: Di- and triblock copolymers of poly(ethylene oxide) and poly(ethyl acrylate), *Langmuir* 20 (2004) 1597–1604.
9. S. Bontha, A.V. Kabanov, T.K. Bronich, Polymer micelles with cross-linked ionic cores for delivery of anticancer drugs, *J. Control. Release* 2006, 114, 163–174
10. T.K. Bronich, P.A. Keifer, L.S. Shlyakhtenko, A.V. Kabanov, Polymer micelle with cross-linked ionic core, *J. Am. Chem. Soc.* 2005, 127, 8236–8237
11. J.O. Kim, N.V. Nukolova, H.S. Oberoi, A.V. Kabanov, T.K. Bronich, Block ionomer complex micelles with cross-linked cores for drug delivery, *Polymer Science Series A* 51 (2009) 708–718.
12. P. Di Bernardo, P.L. Zanonato, S. Tamburini, P. Tomasin, P.A. Vigato, Complexation behaviour and stability of Schiff bases in aqueous solution. The case of an acyclic diimino(amino) diphenol and its reduced triamine derivative, *Dalton Transactions* (2006) 4711–4721.
13. C. Godoy-Alcantar, A.K. Yatsimirsky, J.M. Lehn, Structure-stability correlations for imine formation in aqueous solution, *Journal of Physical Organic Chemistry* 18 (2005) 979–985.